

CYCLIC LOADING TEST FOR WALLS WITH ASPECT RATIO 1.0, 0.5, AND 2.0 WITH GRADE 550 MPa SHEAR REINFORCEMENT

Jang-Woon Baek¹, Hong-Gun Park², Hyun-Mock Shin³, and Sang-Jun Yim⁴

¹ Post-doc., Architecture & Architectural Engineering, Seoul National University, Korea

² Professor, Architecture & Architectural Engineering, Seoul National University, Korea

³ Professor, Civil and Environmental Engineering, Sungkyunkwan University, Korea

⁴ Researcher, Plant Construction & Engineering Laboratory, Korea Hydro & Nuclear Power Central Research, Institute, Korea

ABSTRACT

In the shear design of massive walls in nuclear power plants, high-strength reinforcing bars need to be employed to enhance the constructability and economy of the walls. In the present study, walls with aspect ratios of 1.0, 0.5, and 2.0 were tested under cyclic lateral loading to investigate the effect of 550 MPa reinforcing bars on the shear strength of RC walls. The test parameters included the grade and ratio of shear reinforcement, concrete compressive strength, and the presence of boundary hoops. The ratios of the test shear strength to ACI 349 prediction (i.e., safety margins) were 1.45-2.61 and 1.11-1.74 for the general and seismic provisions, respectively. The test results of walls with 550 MPa re-bars were comparable to those of walls with 420 MPa re-bars for all three evaluations: failure mode, safety margin, and average crack width.

INTRODUCTION

In the construction of nuclear power plants, a number of large diameter reinforcing bars are used in massive reinforced concrete (RC) walls, which significantly affects the constructability and economy. Thus, to enhance the constructability and economy, the use of Grade 550 MPa bars needs to be considered. However, in ACI 349, the use of maximum yield strength of shear reinforcing bars is limited to Grade 420 MPa. Generally, the yield strength of shear bars is limited to ensure 1) to induce yielding of shear reinforcement by limiting the yield, and 2) to control the crack width of potential diagonal shear cracking. In particular, for the use of 550 MPa bars in nuclear power plants walls, which are large portion of nuclear power plant structures, a series of shear wall testing using 550 MPa shear reinforcement is necessary to investigate shear capacity and ductility capacity under cyclic loading.

Many experimental studies (Barda et al., 1977; Cardenas et al., 1973; Hirosawa, 1975; Maier and Thürlimann, 1985; Massone and Wallace, 2004; Sato et al., 1989; Seki et al., 1995) were performed to investigate the shear strength of low-rise walls approximately with $h_w/l_w = 1.0$ ($0.85 \leq h_w/l_w \leq 1.12$). In the majority of the wall specimens, the yield strength f_{yh} of shear reinforcement was less than 550 MPa (295 to 537 MPa). Sato et al. (1989) studied the effect of the yield strength and ratio of shear reinforcement on low-rise walls with a flanged cross section [$h_w/l_w = 0.47$ -1.02, $f'_c = 24, 33$, and 42 MPa, $f_{yh} = 296, 422$, and 528 MPa, and $\rho_h = 0.45\%$ -1.16%]. They reported that when the value of $\rho_h f_{yh}$ was maintained, the yield strength of the shear reinforcement did not affect the shear strength and failure mode of the walls. Lefas et al. (1990) tested walls with high horizontal bar ratios [$h_w/l_w = 1.0$ -2.0, $f'_c = 30.1$ -53.6 MPa, $f_{yh} = 420$ -520 MPa, and $\rho_h = 0.37$ -1.17%]. Despite doubling horizontal bar ratio, the shear strength was not increased. In the case of such high horizontal bar ratios, the specimens failed due to concrete web-crushing, before yielding of the horizontal bars.

In existing studies (Bouchon et al., 2004; Farvashany et al., 2008; Gao, 1999; Gupta and Rangan, 1998; Hirosawa, 1975; Kabeyasawa and Hiraishi, 1998; Maier and Thürlimann, 1985; Nazé and Sidaner, 2001;

Palermo et al., 2002; Saito et al., 1989; Yanagisawa et al., 1992), tests were performed for low-rise walls ($0.33 \leq h_w/l_w \leq 1.17$) with a barbell or flanged cross-section, using high-strength shear re-bars (f_{yh} or $f_{yv} \geq 550$ MPa). In shear failure mode specimens, the test strengths were greater than the ACI 349 predictions, despite the large shear re-bar ratio. Studies for shear reinforcement with higher yield strength of $f_{yh} \geq 550$ MPa are relatively limited for walls with rectangular cross-section, particularly with shear failure mode. On the other hand, tests for intermediate walls and slender walls with high-strength shear reinforcement are rare both in walls with a barbell or flanged cross-section and in walls with a rectangular cross-section: Hirose (1975), Lefas et al. (1990), and Pilakoutas and Elnashai (1995), tested walls with $h_w/l_w = 1.88$ -2.0. However, the yield strength f_{yh} and f_{yv} of shear reinforcement was less than 550 MPa [406.9 - 550 MPa]. Furthermore, owing to the higher aspect ratios of 1.88-2.0, the majority of the test specimens showed flexural yielding before shear failure. Pilakoutas and Elnashai (1995) studied the effect of the amount and distribution of shear reinforcement on the failure mode of the specimens under cyclic lateral loading. However, only a test specimen showed shear failure mode. Pilakoutas and Elnashai (1995) reported that even in flexural mode specimens, shear strength degradation occurred after flexural yielding. Gulec and Whittaker (2011) developed empirical equations to predict the shear strength of low-rise walls ($h_w/l_w \leq 1.0$) with a rectangular cross-section, barbell-shape, or flanged cross-section. For this, statistical analysis was performed on existing test results of 227 walls (74 rectangular, 79 barbell-shaped, and 74 flanged cross-sections). Kassem (2015) developed a closed-form equation of a strut-and-tie model to predict the shear strength of squat walls using existing test results of 664 rectangular and flanged walls ($h_w/l_w \leq 2.0$). However, in these studies, the number of specimens with shear reinforcement greater than 550 MPa was limited.

As such, test results for walls with high reinforcement ratio and high-strength bars are currently limited, particularly for rectangular cross-section walls which are expected to be more vulnerable to shear failure than barbell-shaped walls and flanged walls (Lefas et al., 1990).

In the present study, cyclic lateral loading tests were performed for squat, short, and intermediate walls ($h_w/l_w = 0.5, 1.0, \text{ and } 2.0$) with Grade 420 and 550 MPa re-bars to investigate the effect of Grade 550 MPa re-bars on the shear strength. The major test parameters were the grade and ratio of the shear reinforcement (i.e., horizontal and vertical web re-bars), the failure modes (shear failure before and after flexural yielding), and presence of boundary confinement hoops. The test results were compared with the shear strengths predicted by the current design codes and by other studies.

TEST PLAN

Major Test Parameters

14 wall specimens were prepared for testing: eight specimens with $h_w/l_w = 1.0$, two specimens with $h_w/l_w = 0.5$, and four wall specimens with $h_w/l_w = 2.0$. The main test parameters are summarized in Table 1 and Fig. 1: aspect ratio, sectional shape, compressive strength of concrete, grade and ratio of shear reinforcement (i.e., horizontal and vertical web re-bars), and boundary confinement hoop.

The specimen names indicate the design parameters used for the specimens. The first letters N and H refer to normal-strength reinforcing bars (420 MPa) and high-strength re-bars (550 MPa) used for shear reinforcement, respectively. The second letter S refer to the design failure mode. In this test, all the specimens had shear failure mode by intentionally increasing the flexural reinforcement that was placed at the wall edges. The shear failure mode specimens were tested to investigate the magnitude of shear strength. In other papers (Baek et al., 2017; Park et al., 2015), the flexural yielding mode specimens were also tested to investigate the effect of Grade 550 MPa shear reinforcement on the shear strength degradation and wall ductility after flexural yielding. The numbers '1', '0.5', and '2' indicate the ratio of wall height to wall length (aspect ratio $h_w/l_w = 1.0, 0.5, \text{ and } 2.0$ in Figs. 1(a), 1(c), and 1(e), respectively). The third letters indicate the horizontal re-bar ratio: M, T, H, and O refer to 100%, 67%, 50%, and 33% (maximum, two third, a half, and one third) of the permissible shear reinforcement ratio, respectively, where the permissible shear reinforcement was calculated using $V_s = V_{smax}$ [the design shear strength contributed by shear reinforcement = the permissible maximum shear strength by shear reinforcement].

The last letter H or B following dash (-), if any, indicates additional details: H refers to high-strength concrete (compressive strength of concrete $f'_c = 70$ MPa); and B refers to the use of boundary confinement hoops for flexural mode specimens. For example, HS1O-B indicates a shear mode specimen with Grade 550 MPa shear reinforcing bars, aspect ratio of 1.0, one third of maximum shear reinforcement ratio, and boundary confinement hoops at the wall edges.

Table 1. Design parameters of shear failure mode specimens

Specimens	Wall dimension ($h_w \times l_w$) (mm×mm)	Concrete strength, f'_c (MPa) [Compressive load, P (kN)]	Reinforcement										$V_n^{(3)}/V_f^{(4)}$
			Web					Boundary region					
			Horizontal				Vertical		Vertical		Hoop		
			$V_s^{(1)}/V_{smax}^{(2)}$	f_{yh} (MPa)	ρ_h (%)	$\rho_h f_{yh}$ (MPa)	f_{yv} (MPa)	ρ_v (%)	f_{yf} (MPa)	ρ_f (%)	f_{ysf} (MPa)	ρ_s (%)	
NS1M	1500 × 1500	52.9 [1060]	0.90	470	0.93	4.36	470	1.10	617	9.57	-	-	2.25
HS1M		52.9 [1060]	0.93	667	0.68	4.51	667	0.70	617	9.57	-	-	2.16
NS1T		46.5 [970]	0.71	477	0.68	3.22	653	0.66	617	9.57	-	-	2.51
HS1T		46.5 [970]	0.74	667	0.51	3.38	653	0.66	617	9.57	-	-	2.50
HS1T-H		70.3 [1470]	0.60	667	0.51	3.38	653	0.66	617	9.57	-	-	2.73
HS1O		46.1 [970]	0.37	667	0.25	1.69	653	0.36	617	9.57	-	-	2.84
HS1O-H		70.3 [1470]	0.30	667	0.25	1.69	653	0.36	617	9.57	-	-	3.13
HS1O-B		46.5 [970]	0.37	667	0.25	1.69	653	0.36	617	9.57	667	5.32	2.82
NS0.5M	750 × 1500	44.6 [845]	0.98	470	0.93	4.36	470	0.92	617	9.57	-	-	2.13
HS0.5M		37.4 [720]	1.11	667	0.68	4.51	667	0.58	617	9.57	-	-	1.97
NS2M	3000 × 1500	36.5 [720]	1.08	470	0.93	4.36	470	1.10	617	12.75	-	-	1.51
HS2M		36.5 [720]	1.12	667	0.68	4.51	667	0.56	617	12.75	-	-	1.44
NS2H		36.5 [720]	0.54	470	0.46	2.18	470	0.66	617	9.57	-	-	1.97
HS2H		36.5 [720]	0.56	667	0.34	2.25	667	0.42	617	9.57	-	-	1.91

¹⁾ V_s = Predicted contribution of shear reinforcement in ACI 349, ²⁾ V_{smax} = Maximum shear strength contributed by shear reinforcement using V_c , ³⁾ V_n = Shear strength prediction in ACI 349, ⁴⁾ V_f = Flexural strength prediction.

Test set-up

Axial compressive loading and lateral cyclic loading were applied using the test set-up shown in Fig. 2. An axial load of approximately $0.07A_c f'_c$ (970 kN for 46 MPa concrete, and 1470 kN for 70 MPa concrete), was applied at the top of the wall by two displacement-controlled actuators. The level of the axial compressive force was maintained during cyclic lateral loading, by manually controlling the vertical displacement (See Fig. 2(a)). The lateral loading protocol followed the “Acceptance Criteria for Special Structural Walls (Hawkins and Ghosh, 2003)”, as shown in Fig. 2(b). Fig. 2(a) shows the linear variable differential transformers (LVDTs) for the measurement of lateral displacements, sliding at the base, and shear deformations. Figs. 1(a), 1(c), and 1(e) show the strain gauges, to measure the strains of the flexural bars, web vertical bars, and horizontal bars.

TEST RESULTS

Damages and Failure Modes

To directly compare the failure modes of specimens with Grade 420 and 550 MPa shear reinforcement, Fig. 3 shows the failure modes of the specimens at the end of the tests. Table 2 summarize the failure modes. Generally, the failure modes of the specimens with Grade 550 MPa bars were similar to those of the specimens with Grade 420 MPa bars.

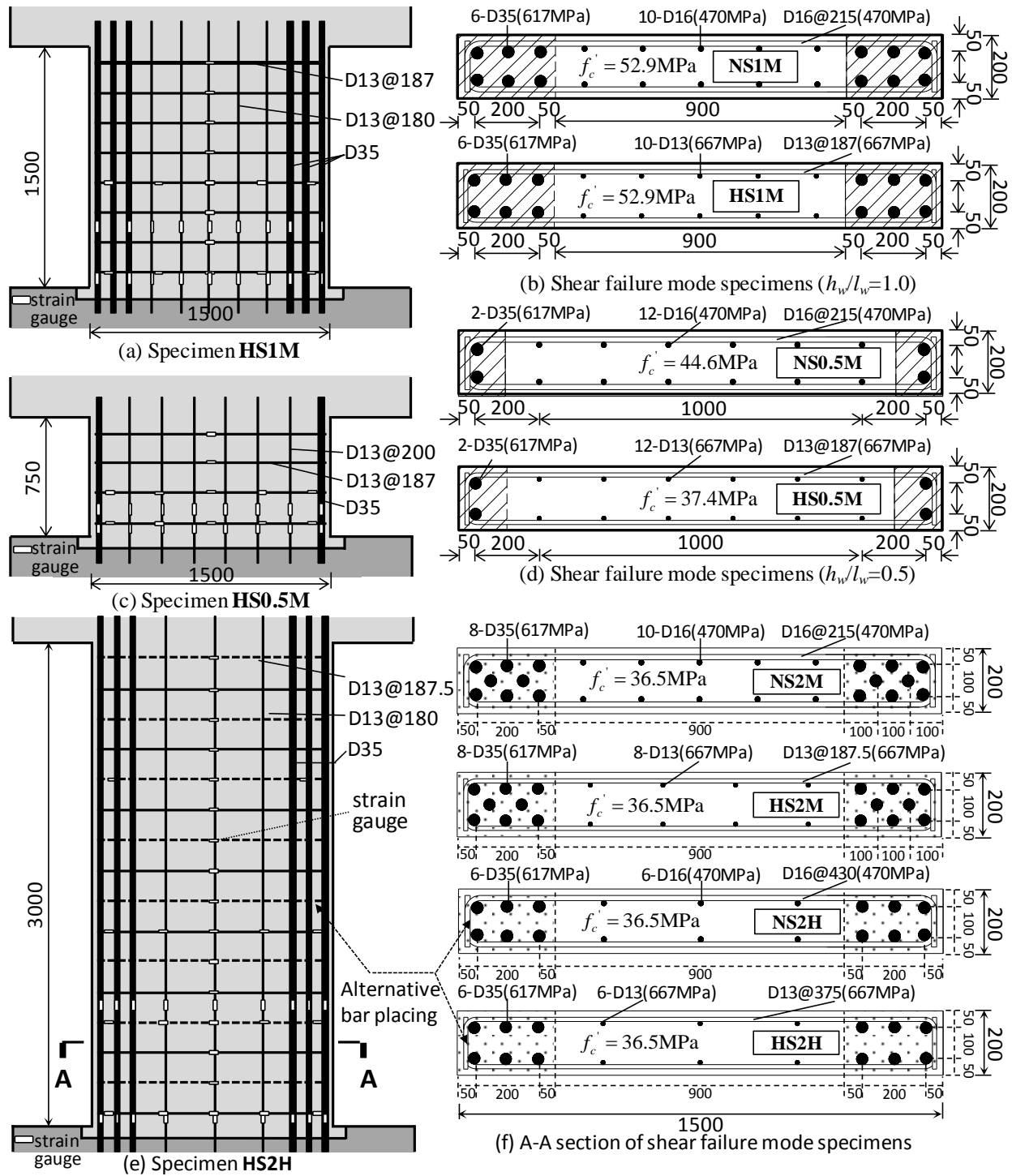


Fig. 1. Dimensions and reinforcement details of specimens

NS1M and HS1M (Figs. 3(a) and 3(b)) with the ACI 349-specified maximum shear strength $V_{n,max}$ failed due to a mixed mode of diagonal tension cracking and diagonal web crushing (DT+WC). In Figs. 3(c) and 3(d), the failure modes of NS0.5M and HS0.5M, and were similar to those of NS1M (or HS1M) (DT+WC). The results indicate that the use of higher yield strength re-bars (Grade 550 MPa re-bars) did

not affect the failure mode. NS2M and HS2M (Figs. 3(e) and 3(f)) with the maximum shear reinforcement ratio ρ_{hmax} failed owing to diagonal web crushing (WC). NS2H and HS2H (Figs. 3(g) and 3(h)) with $0.5\rho_{hmax}$ failed owing to diagonal tension cracking (DT).

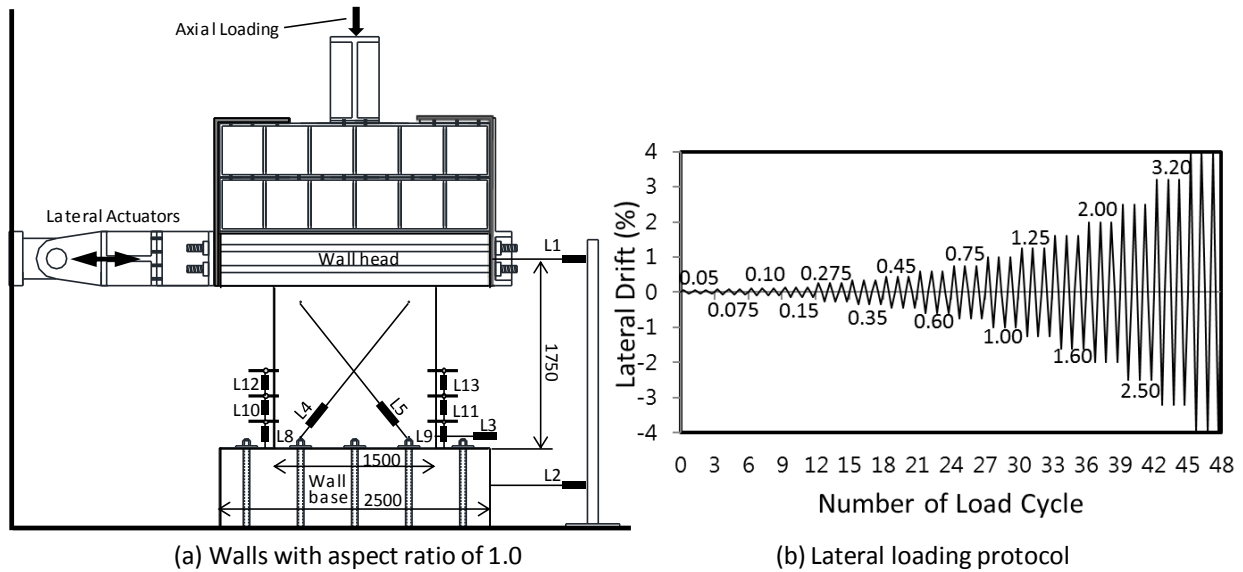


Fig. 2. Test set-up and lateral loading protocol

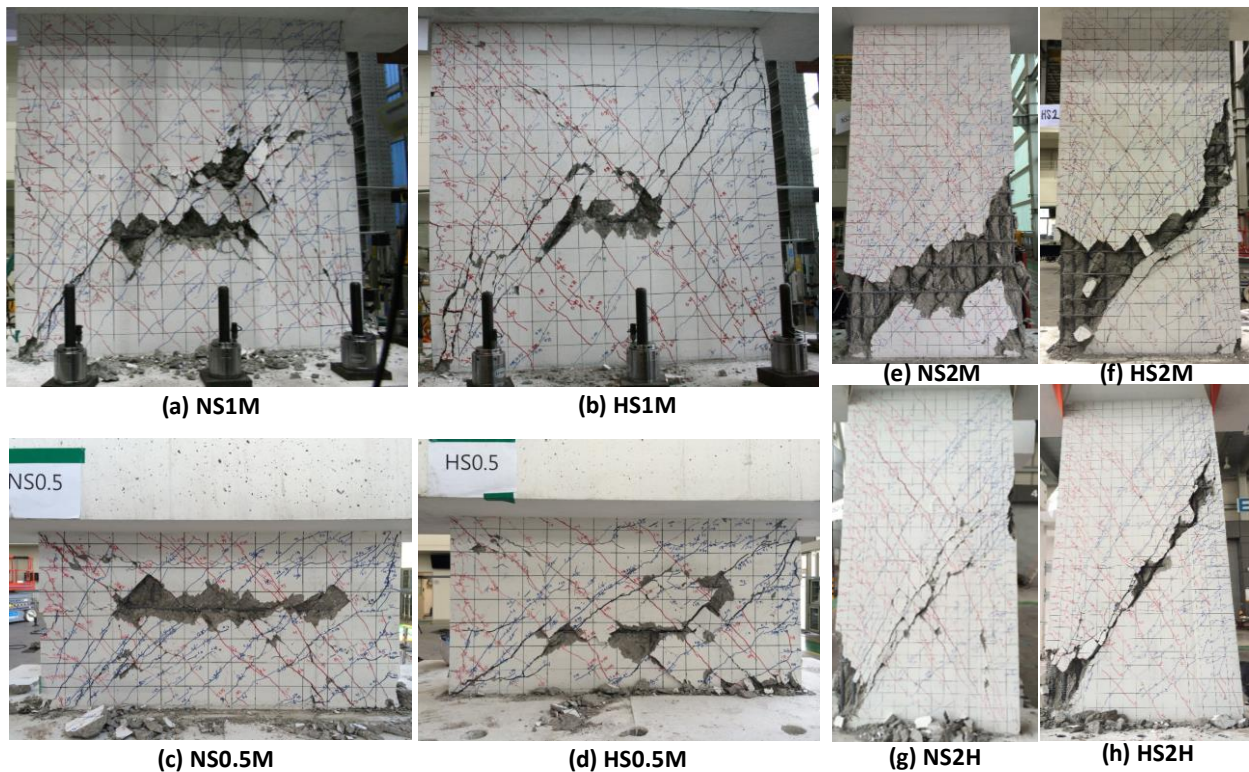


Fig. 3. Damage modes of specimens

Table 2. Test results of shear failure mode specimens and strength prediction

Specimens	$V_f^{1)}$ (kN)	Test results					Ratio of test strengths to predictions				
		$V_{test,s}^{2)}$ (kN)	$V_{test,g}^{2)}$ (kN)	$V_{test}^{2)}$ (kN)	Drift ratio at V_{test} (%)	Failure mode ³⁾	ACI 349 general provision	ACI 349 seismic provision	ASCE 2005	Wood	Gulec
							$V_{test,s}/V_n$	$V_{test,s}/V_{seis}$	$V_{test,s}/V_{ASCE}$	$V_{test,s}/V_{Wood}$	$V_{test,s}/V_{Gulec}$
NS1M	2994	2275	2360	2318	+1.30/-1.30	WC+DT	1.71	1.23	1.14	1.25	1.25
HS1M	2958	2111	2176	2144	+1.15/-1.20		1.54	1.11	1.01	1.16	1.16
NS1T	2621	2265	2332	2298	+1.00/-1.00	WCS+DT	2.17	1.53	1.16	1.33	1.33
HS1T	2712	2130	2187	2158	+1.00/-1.00		1.97	1.40	1.05	1.25	1.25
HS1T-H	3131	2108	2135	2121	+0.75/-0.75		1.84	1.28	0.91	1.07	1.01
HS1O	1925	1468	1488	1478	+1.00/-1.00	WCS+DT	2.17	1.45	0.72	1.12	0.87
HS1O-H	2319	1822	1931	1877	+1.00/-1.00		2.46	1.60	0.78	1.39	0.94
HS1O-B	1915	1772	2060	1916	+0.90/-0.90	WC+DT	2.61	1.74	0.87	1.35	1.05
NS0.5M	2791	2492	2572	2532	+1.35/-1.20	WC+DT	1.90	1.38	1.41	2.49	1.49
HS0.5M	2611	2351	2504	2428	+1.50/-1.00		1.77	1.30	1.32	2.56	1.54
NS2M	1940	1990	2043	2016	+2.10/-2.10	WC	1.55	1.24	1.13	1.32	1.32
HS2M	1909	1919	2000	1960	+2.45/-2.05		1.45	1.16	1.08	1.27	1.27
NS2H	1500	1311	1362	1336	+1.60/-1.40	DT	1.72	1.37	0.96	0.87	0.90
HS2H	1491	1416	1446	1431	+1.55/-1.25		1.81	1.45	1.03	0.94	0.97

¹⁾ V_f = flexural strength prediction. ²⁾ $V_{test,s}$, $V_{test,g}$, and V_{test} = the smaller, greater, and average values of the measured maximum loads in the positive and negative loading directions, respectively. ³⁾ WCS is web crushing after sliding, WC is web crushing without sliding, DT is diagonal tension failure.

Lateral Load-displacement Relationships

In the shear failure mode specimens with both Grade 550 MPa and Grade 420 MPa re-bars, the test shear strengths V_{test} were greater than the predictions of the ACI 349 (ACI 318) general and seismic provisions. The strength ratios of the specimens with Grade 550 MPa web re-bars ($[V_{test,s}/V_n = 1.54$ (HS1M), 1.77 (HS0.5M), 1.45 (HS2M), 1.97 (HS1T), 1.81 (HS2H)]) were slightly less than those of the specimens with Grade 420 MPa web re-bars [$V_{test,s}/V_n = 1.71$ (NS1M) and 1.90 (NS0.5M), 1.55 (NS2M), 2.17 (NS1T), 1.72 (NS2H)]. Further, the strength ratios of the walls decreased as the wall aspect ratio h_w/l_w increased and the effective re-bar strength $\rho_{hf}f_{yh}$ increased. Nevertheless, the lateral load-displacement relationships of walls with Grade 550 MPa shear re-bar were generally similar to those with Grade 420 MPa re-bars.

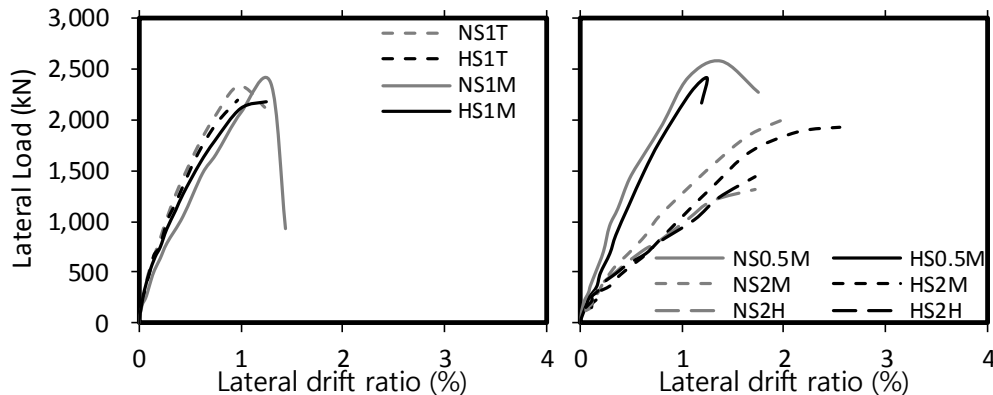


Fig. 4. Envelop curves of specimens

Average Diagonal Crack Width

The average diagonal crack width was estimated using the length change measured by the diagonal LVDTs in the wall panels (L4-L5 in Fig. 2(a)): The average diagonal crack width was calculated by dividing the maximum length change by the number of diagonal cracks at each loading step. The results are shown in Fig. 5.

The permissible crack width recommended by ACI 318-14 under service load was also marked (0.41 mm). The service load can be regarded as about 60% of the ultimate strength. The average diagonal crack width of the specimens with Grade 550 MPa re-bars was similar to the counterpart specimens with Grade 420 MPa re-bars.

In the specimens with $h_w/l_w = 1.0$ (Fig. 5(a)), the average diagonal crack width reached the ACI permissible crack width 0.41 mm at the service load ($0.6V_{test}$). On the other hand, in the specimens with $h_w/l_w = 0.5$, the average diagonal crack width was less than 0.41 mm until the service load (Fig. 5(b)). The average diagonal crack widths of NS2H and HS2H with the smaller effective shear reinforcement strength $\rho_h f_{yh}$ were greater than those of NS2M and HS2M (Fig. 5(c)). At the ultimate loading, the average crack width of NS2H was the greatest, because the spacing of web horizontal bars was the greatest among the specimens; the spacing of the horizontal web bars in NS2H was 55 mm greater than that of HS2H. This result indicates that in the case of 420 and 550 MPa bars, the width of diagonal cracks increases as the effective shear reinforcement strength $\rho_h f_{yh}$ decreases and the spacing of shear reinforcement increases, and the crack width is not directly related to the bar steel grade.

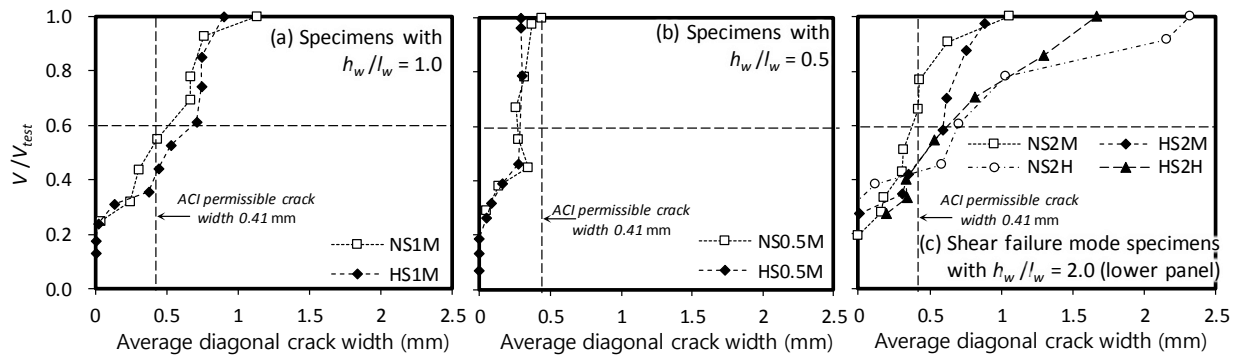


Fig. 5. Average diagonal crack width of test specimens

Shear Strength Prediction by Existing Design Methods

In Fig. 6, the test shear strengths of the specimens with $h_w/l_w = 1.0$, 0.5, and 2.0 in the present study are compared with test results of previous studies. The shear strengths of the existing wall specimens with rectangular cross-section (Cardenas et al., 1973; Greifenhagen and Lestuzzi, 2005; Hirose, 1975; Pilakoutas and Elnashai, 1995; Salonikios et al., 1999) and specimens with barbell-shaped or flanged walls (Barda et al., 1977; Burgueño et al., 2014; Farvashany et al., 2008; Fukuzawa et al., 1988; Hirose, 1975; Huang and Sheu, 1988; Kabeyasawa and Hiraishi, 1998; Maier and Thürlimann, 1985; Mo and Chan, 1996; Palermo et al., 2002; Saito et al., 1989; Sato, Ogata, Suzuki, et al., 1989; Seki et al., 1995; Sugano, 1991; Yanagisawa et al., 1992) were evaluated using Eqs. (3 1), (3 2), and (3 5). The maximum permissible shear strength $V_{max} (= 0.83\sqrt{f_c'}hd)$ was applied. The aspect ratio h_w/l_w of the existing wall specimens with for rectangular cross-section and with barbell-shaped or flanged cross-section ranged from 0.5 to 2.0 and from 0.21 to 2.25, respectively.

Fig. 7 shows the safety margins (i.e. the strength ratio) of the test specimens predicted by the ACI 349 or ACI 318 general and seismic provisions [(ACI Committee 349, 2013) or (ACI Committee 318, 2014)], ASCE 43-05 (Nuclear Standards Committee, 2005), Wood (1990), and Gulec and Whittaker (2011). In

the provisions of ACI 349 (ACI 318) [general and seismic provisions], the strength ratio decreased as $\rho_h f_{yh}$ increased (Figs. 6(a) and 6(b)). This is because ACI 349 does not include the shear contribution of vertical web re-bars in the strength predictions [In the specimens, the ratio of vertical re-bars increased with the ratio of horizontal re-bars.]. Nevertheless, the strength ratios of the specimens with the maximum shear reinforcement ratio were greater than 1.0, for both using Grade 420 and 550 MPa shear re-bars. On the other hand, the predictions by ASCE 43-05, and Gulec and Whittaker (V_{test}/V_{ASCE} and V_{test}/V_{Gulec}) slightly increased as $\rho_h f_{yh}$ increased, and showed better predictions than the other predictions, regardless of h_w/l_w and $\rho_h f_{yh}$. The methods address the shear-contribution of vertical re-bars varying with wall aspect ratios (Figs. 6(c) and 6(e)). In the case of the predictions by the ACI 349 general provision and Wood, the safety margin of the walls with $h_w/l_w = 0.5$ was greater than that of the other methods (Figs. 6(a) and 6(d)) because the methods do not address the effect of the aspect ratio h_w/l_w .

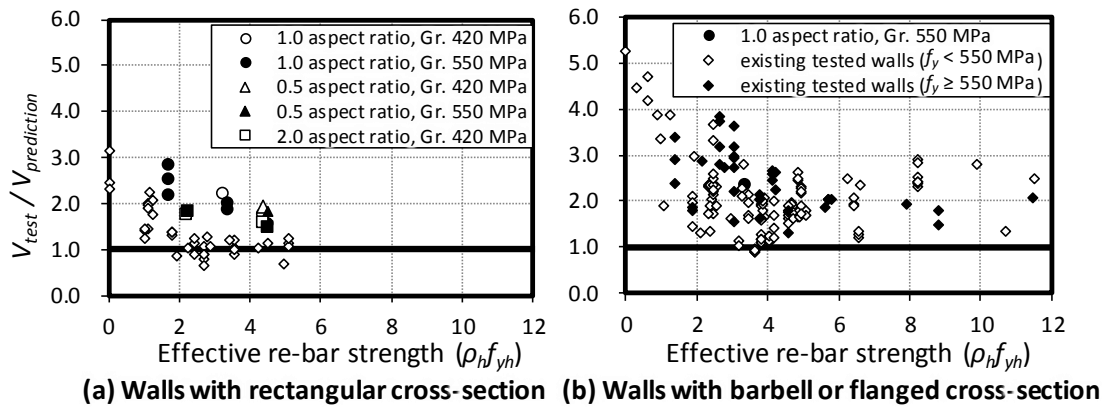


Fig. 6. Comparison of experimental shear strengths and predictions by the ACI 349 general provision

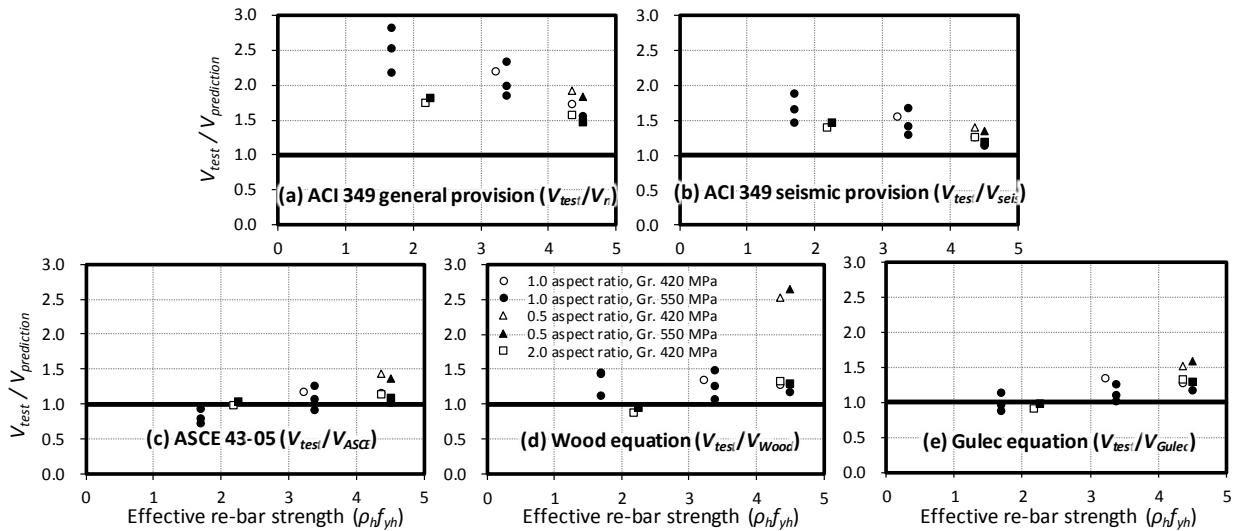


Fig. 7. Comparison of test shear strengths and predictions

CONCLUSION

To investigate the validity of Grade 550 MPa bars for shear reinforcement of walls, eight, two, and four wall specimens with aspect ratio $h_w/l_w = 1.0, 0.5,$ and $2.0,$ respectively, were tested under cyclic lateral loading. The test results of the walls with Grade 550 MPa web bars were directly compared with those of walls with Grade 420 MPa web bars. Shear failure mode specimens were tested to investigate the effect of

Grade 550 MPa bars on the shear strength before flexural yielding. The major findings of the present study are summarized as follows.

1. The shear failure mode specimens with the ACI 349 code-specified maximum shear strength $V_{n,max}$ failed due to diagonal web crushing (WC), with [in the case of $h_w/l_w \leq 1.0$] or without [in the case of $h_w/l_w = 2.0$] diagonal tension cracking (DT). In the case of moderate height walls with smaller shear reinforcement ratio, diagonal tension failure (DT) occurred.
2. In the shear failure mode specimens with Grade 550 MPa re-bars, the test shear strengths V_{test} were greater than the predictions of the ACI 349 (ACI 318) general and seismic provisions. The strength ratios of the specimens with Grade 550 MPa web re-bars were slightly less than those of the specimens with Grade 420 MPa web re-bars. Further, the strength ratios of the walls decreased as the wall aspect ratio h_w/l_w increased and the effective re-bar strength ρ_{lfy_h} increased.
3. In the case of walls with Grade 420 or 550 MPa re-bars, the number of diagonal shear cracks was not directly related to the re-bar grade. The average diagonal crack width was related to the effective shear reinforcement strength ρ_{lfy_h} rather than the re-bar grade when the spacings of the shear reinforcement were the same.
4. The test shear strengths were compared with test results of previous studies that used high- or moderate-strength shear reinforcing bars. The result showed that the trend of the test results of the present study is similar to that of the previous studies: the strength ratios by ACI 349 (or ACI 318) decreased as the ρ_{lfy_h} increased; and the strength ratios of the specimens tested in the present study were comparable to those of the existing test specimens.
5. The strength predictions by ASCE 43-05, and Gulec and Whittaker were better than those by other methods, regardless of h_w/l_w and ρ_{lfy_h} , because the methods address the shear-contribution of vertical re-bars varying with wall aspect ratios. In the predictions by the ACI 349 general provision and Wood, the safety margin of the walls with $h_w/l_w = 0.5$ was greater than that of other methods, because the methods do not address the effect of the aspect ratio h_w/l_w .
6. The test results showed that the overall behaviors of the walls with Grade 550 MPa shear re-bars were similar to those of the walls with Grade 420 MPa shear re-bars.

ACKNOWLEDGEMENTS

This work was supported by Korea Hydro & Nuclear Power Co. Ltd (No. L16S140000).

REFERENCES

- ACI Committee 318 (2014). Building Code Requirements for Structural Concrete (ACI 318-14) and Commentary. *American Concrete Institute*, Farmington Hills, MI, p. 520.
- ACI Committee 349 (2013). Code Requirements for Nuclear Safety-Related Concrete Structures (ACI 349-13) and Commentary. *American Concrete Institute*, Farmington Hills, MI, p. 196.
- Baek, J. W., Park, H. G., Shin, H. M., and Yim, S. J. (2017). Cyclic Loading Test for Reinforced Concrete Walls (Aspect Ratio 2.0) with Grade 550 MPa (80 ksi) Shear Reinforcing Bars. *ACI Structural Journal*, 114(3), pp. 673.
- Barda, F., Hanson, J. M., and Corley, W. G. (1977). Shear Strength of Low-rise Walls with Boundary Elements. *ACI Special Publication*, 53, pp. 149-202.
- Bouchon, M., Orbovic, N., and Foure, N. (2004). Tests on Reinforced Concrete Low-rise Shear Walls under Static Cyclic Loading. *the 13th World Conference on Earthquake Engineering(257)*
- Cardenas, A. E., Hanson, J. M., Corley, W. G., and Hognestad, E. (1973). Design Provisions for Shear Walls. *ACI Journal Proceedings*, 70(3), pp. 221-230.
- Farvashany, F. E., Foster, S. J., and Rangan, B. V. (2008). Strength and Deformation of High-strength Concrete Shearwalls. *ACI Structural Journal*, 105(1), pp. 21.
- Gao, X. (1999). Framed Shear Walls under Cyclic Loading. (PhD thesis), *Department of Civil and Environmental Engineering, University of Houston*, Houston, TX, p. 285.

- Gulec, C. K. and Whittaker, A. S. (2011). Empirical Equations for Peak Shear Strength of Low Aspect Ratio Reinforced Concrete Walls. *ACI Structural Journal*, 108(1), pp. 80-89.
- Gupta, A. and Rangan, B. V. (1998). High-strength Concrete (HSC) Structural Walls. *ACI Structural Journal*, 95(2), pp. 194-204.
- Hawkins, N. M. and Ghosh, S. K. (2003). Acceptance Criteria for Special Structural Walls Based on Validation Testing: Proposed Provisional Standard and Commentary, SK Ghosh Associates Inc., Northbrook, IL.
- Hirosawa, M. (1975). Past Experimental Results on Reinforced Concrete Shear Walls and Analysis on Them (in Japanese). *Building Research Institute, Ministry of Construction*, Tokyo, Japan, p. 277.
- Kabeyasawa, T. and Hiraishi, H. (1998). Tests and Analyses of High-strength Reinforced Concrete Shear Walls in Japan. *ACI Special Publication*, 176, pp. 281-310.
- Kassem, W. (2015). Shear Strength of Squat Walls: A Strut-and-tie Model and Closed-form Design Formula. *Engineering Structures*, 84, pp. 430-438.
- Lefas, I. D., Kotsovos, M. D., and Ambraseys, N. N. (1990). Behavior of Reinforced Concrete Structural Walls: Strength, Deformation Characteristics, and Failure Mechanism. *ACI Structural Journal*, 87(1), pp. 23-31.
- Maier, J. and Thürlimann, B. (1985). Bruchversuche an Stahlbetonscheiben (in German). *Institut für Baustatik und Konstruktion, Eidgenössische Technische Hochschule (ETH) Zürich*, Zürich, Switzerland, p. 130.
- Massone, L. M. and Wallace, J. W. (2004). Load-deformation Responses of Slender Reinforced Concrete Walls. *ACI Structural Journal*, 101(1), pp. 103-113.
- Nazé, P. A. and Sidaner, J. F. (2001). Presentation and Interpretation of SAFE Tests: Reinforced Concrete Walls subjected to Shearing. *the 16th International Conference on Structural Mechanics in Reactor Technology*(1084), Washington, DC, pp. 1-12.
- Nuclear Standards Committee (2005). Seismic Design Criteria for Structures, Systems, and Components in Nuclear Facilities. *American Society of Civil Engineers*, Reston, VA, p. 81.
- Palermo, D., Vecchio, F. J., and Solanki, H. (2002). Behavior of Three-dimensional Reinforced Concrete Shear Walls. *ACI Structural Journal*, 99(1), pp. 81-89.
- Park, H. G., Baek, J. W., Lee, J. H., and Shin, H. M. (2015). Cyclic Loading Tests for Shear Strength of Low-Rise Reinforced Concrete Walls with Grade 550 MPa Bars. *ACI Structural Journal*, 112(3), pp. 299-310.
- Pilakoutas, K. and Elnashiai, A. (1995). Cyclic Behavior of Reinforced Concrete Cantilever Walls, Part 1: Experimental Results. *ACI Structural Journal*, 92(3), pp. 271-281.
- Saito, H., Kikuchi, R., Kanechika, M., and Okamoto, K. (1989). Experimental Study on the Effect of Concrete Strength on Shear Wall Behavior. *Tenth International Conference on Structural Mechanics in Reactor Technology*, H08/05, Anaheim, CA, pp. 227-232.
- Sato, S., Ogata, Y., Yoshizaki, S., Kanata, K., Yamaguchi, T., Nakayama, T., Inada, Y., and Kadoriku, J. (1989). Behavior of Shear Wall Using Various Yield Strength of Rebar, Part 1: An Experimental Study. *Tenth International Conference on Structural Mechanics in Reactor Technology*, H09/01, Anaheim, CA, pp. 233-238.
- Seki, M., Kobayashi, J., Shibata, A., Kubo, T., Taira, T., and Akino, K. (1995). Restoring Force Verification Test on Shear Wall. *Thirteenth International Conference on Structural Mechanics in Reactor Technology*, H06-1, Porto Alegre, Brazil, pp. 39-44.
- Wood, S. L. (1990). Shear Strength of Low-rise Reinforced Concrete Walls. *ACI Structural Journal*, 87(1), pp. 99-107.
- Yanagisawa, N., Kamide, M., and Kanoh, Y. (1992). Study on High Strength Reinforced Concrete Shear Walls : Part1. Outline of tests (in Japanese). *Summaries of technical papers of Annual Meeting Architectural Institute of Japan: Structures II*, Japan, pp. 347-348.